Ulgen, D. *et al*. (2015) ***Géotechnique Letters*** **5**, 261–268, http://dx.doi.org/10.1680/jgele.15.00097

# Assessment of racking deformation of rectangular underground structures by centrifuge tests

D. ULGEN*, S. SAGLAM† and M. Y. OZKAN‡

Seismic safety of buried structures has become increasingly important over the past two decades, especially after the destructive earthquakes such as in Kobe, Japan (1995), Kocaeli, Turkey (1999) and Chi-Chi, Taiwan (1999). Some of the embedded structures including pipelines, subways and tunnels collapsed or suffered severe damage in those earthquakes due to inappropriate design. The main difficulty in seismic design is the incorporation of soil–structure interaction effect governed by the relative stiffness (flexibility ratio) between the soil and the embedded structure. This study aims to clarify the effect of flexibility ratio on the dynamic response of rectangular structures buried in dry sand. For that purpose, a series of dynamic centrifuge tests were conducted on two types of box-shaped models with different rigidities under various harmonic motions. The results reveal that the magnitude of dynamic lateral earth pressure and sidewall deformation is highly dependent on the flexibility ratio of the embedded structure. Based on the flexibility ratios, racking deformations observed in centrifuge tests and racking deformations estimated through analytical approaches were evaluated in a comparative manner.

**KEYWORDS:** buried structures; centrifuge modelling; dynamics



## NOTATION

| | |
|---|---|
| $D$ | damping ratio |
| $D_{50}$ | mean particle diameter |
| $e$ | void ratio |
| $F$ | flexibility ratio |
| $G$ | shear modulus |
| $G_{\mathrm{m}}$ | degraded shear modulus |
| $G_{\max}$ | maximum shear modulus |
| $H$ | height of the underground structure model |
| $k$ | overconsolidation ratio exponent |
| $k_{\mathrm{d}}$ | dynamic lateral pressure coefficient |
| $P_{\mathrm{d}}$ | maximum pressure value of triangular pressure distribution |
| $R$ | racking ratio |
| $R_D$ | relative density |
| $\boldsymbol{S}$ | force required to enable unit racking deformation |
| $W$ | width of the underground structure model |
| $\gamma$ | shear strain |
| $\Delta_{\mathrm{ff}}$ | free-field deformation |
| $\Delta_{\mathrm{str}}$ | racking deformation of the underground structure |
| $\sigma'_{\mathrm{m}}$ | effective confining pressure |
| $\sigma'_{\mathrm{v,mid}}$ | overburden pressure at mid-depth of the tunnel |

## INTRODUCTION

Experiences gained through the large earthquakes such as in Kobe, Japan (1995), Kocaeli, Turkey (1999) and Chi-Chi, Taiwan (1999) show that underground structures have suffered significant damage due to seismic loading (Sitar, 1995; Iida *et al.*, 1996; Power *et al.*, 1998; Kaneshiro *et al.*, 2000; Hashash *et al.*, 2001; Wang *et al.*, 2001). These damages are mostly caused by fault actions, slope failures, liquefaction-induced floatation or sinking and by racking or ovaling deformations (Wang, 1993, Hashash *et al.*, 2001). Racking type of deformations, common in most rectangular underground structures exposed to seismic loads, are produced due to transverse shear waves (Penzien, 2000). There are two main approaches to estimate the racking deformation of rectangular underground structures. In the free-field approach, the structure is assumed to adapt the deformations of the surrounding soil. Due to ignorance of relative stiffness between soil and structure, racking deformations of the underground structure may be underestimated or overestimated (St. John & Zahrah, 1987; Hashash *et al.*, 2001). Nevertheless, Wang (1993), Penzien (2000), Huo *et al.* (2006) and Bobet *et al.* (2008) proposed simplified frame analysis methodologies in which the soil–structure interaction effect is considered.

O'Rourke *et al.* (2003) and Ha *et al.* (2010) investigated faulting effects on buried pipelines through centrifuge testing. Ling *et al.* (2003) and Chian & Madabhushi (2012) performed centrifuge tests to explore the dynamic behaviour of underground structures in liquefied soils. Moreover, underground structures that have undergone ovaling deformations under vertically propagated shear waves were investigated by means of centrifuge testing (Cilingir & Madabhushi, 2011a, 2011b; Lanzano *et al.*, 2012). In these studies, circular tunnels were addressed with an interest mainly focused on the accelerations in the soil, dynamic earth pressures and the effect of depth on the seismic performance. There are only a few studies (e.g. Cilingir & Madabhushi, 2011c; Dashti *et al.*, 2013; Pitilakis *et al.*, 2013) that have dealt with the dynamic behaviour of rectangular underground structures using the centrifuge technique and the mechanism dominating structural deformations and straining in the soil has been scarcely touched upon. Moreover, extending the current experimental knowledge regarding the dynamic response of rectangular underground structures, it is aimed to provide a stimulating guide for the preliminary seismic assessment of these structures. Centrifuge tests were conducted on aluminium box-shaped

Manuscript received 2 July 2015; accepted 19 October 2015. Published online at www.geotechniqueletters.com on 18 November 2015.
*Department of Civil Engineering, Mugla Sitki Koçman University, Mugla, Turkey
†Department of Civil Engineering, Adnan Menderes University, Aydın, Turkey
‡Department of Civil Engineering, Middle East Technical University, Ankara, Turkey

models embedded in dry sand. Racking deformations measured during the tests have been compared with the estimations of analytical approaches proposed by Penzien (2000) and Bobet *et al.* (2008). The effect of difference in stiffness of the structure and the surrounding soil on the racking deformation has been examined. Consequently, the effect of relative stiffness on the load–deformation mechanism of the sidewalls has been presented.

## DYNAMIC CENTRIFUGE MODELLING

Centrifuge tests were carried out at the IFSTTAR (Institut français des sciences et technologies des transports, de l'aménagement et des réseaux) Centrifuge Laboratory located in Nantes, France. The model was shaken through a cyclic excitation applied at the base of the soil container. Among the alternatives of soil container, equivalent shear beam (ESB) box was preferred to minimise the dynamic boundary effects. It has been verified that the ESB box can be efficiently used to simulate horizontal shear deformations and the semi-infinite soil medium (Madabushi, 1994; Zeng & Schofield, 1996; Teymur & Madabhushi, 2003; Lee *et al.*, 2013).

### *Model ground*

Dry Fontainebleau sand composed of uniform fine quartz constitutes the model ground. The physical properties of the sand are presented in Table 1. The sand was filled in the container using air pluviation technique. To provide a homogeneous soil, the soil particles were dropped from a fixed height of 60 cm. Measurements obtained from the density control boxes and cone penetration tests indicate that homogeneous and reproducible model grounds with a relative density of 70% were achieved in the centrifuge tests. Accordingly, maximum shear modulus, $G_{max}$, at the mid-depth of the culvert model is estimated as 56 500 kPa using the empirical relationship (equation (1)) proposed by Hardin & Drnevich (1972). Li *et al.* (2013) reported the dynamic properties of Fontainebleau sand that were investigated through centrifuge testing. In their study, centrifuge test data were fitted to general empirical equations developed by Ishibashi & Zhang (1993). The shear modulus degradation curves constructed for the Fontainebleau sand were adopted. The shear modulus degradation ($G/G_{max}$) and damping ratio ($D$) were calculated according to the empirical formulae (equations (2)–(4)) proposed in that study

$$G_{max} = 3230\frac{(2{\cdot}973 - e)^2}{(1+e)}\mathrm{OCR}^k(\sigma'_m)^{1/2} \quad (1)$$

where $G_{max}$ is the maximum shear modulus in kPa; $e$ is the void ratio; OCR is the ratio of the maximum experienced effective stress to the present effective stress; $k$ is an over-consolidation ratio exponent and $\sigma'_m$ is the effective confining pressure in kPa

$$\frac{G}{G_{max}} = K(\gamma)\sigma_c^{m(\gamma)-m_0} \quad (2)$$

$$K(\gamma) = 0{\cdot}5\left[1 + \tan h\left\{\ln\left(\frac{0{\cdot}000102}{\gamma}\right)^{0{\cdot}613}\right\}\right] \quad (3)$$

$$m(\gamma) - m_0 = 0{\cdot}34\left[1 - \tan h\left\{\ln\left(\frac{0{\cdot}000556}{\gamma}\right)^{0{\cdot}4}\right\}\right] \quad (4)$$

where $\gamma$ is the shear strain.

**Table 1.** Physical properties of Fontainebleau sand

| | |
|---|---|
| Minimum void ratio | 0·55 |
| Maximum void ratio | 0·86 |
| Minimum unit weight: kN/m$^3$ | 13·93 |
| Maximum unit weight: kN/m$^3$ | 16·78 |
| Unit weight when $R_D = 70\%$ | 15·82 |
| Mean diameter ($D_{50}$): mm | 0·20 |

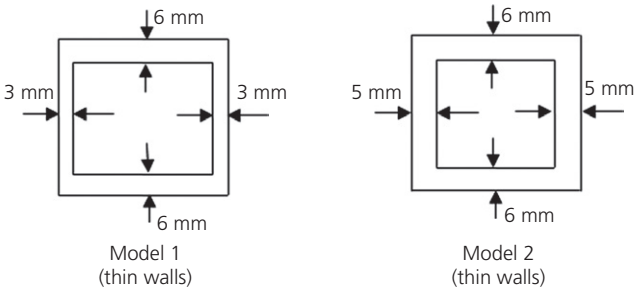


**Fig. 1.** Cross-sections of underground structure models

### *Rectangular underground structure models*

Two underground structure models with different rectangular cross-sections were manufactured using electroerosion technology. This technology makes it possible to avoid stress concentrations, discontinuity and particularly prestressing in the aluminium models. Internal dimensions of these models were kept constant for the purpose of simplicity in instrumentation, whereas the thickness of the sidewalls was modified to obtain different rigidities. To eliminate the bending effects, roof and invert slab were kept relatively thick and stiff compared with that of sidewalls. Cross-sections and dimensions of the models are given in Fig. 1 and Table 2, respectively.

The interface between the tunnel and the ESB box was designed to provide free movement at tunnel ends. Figure 2 shows the photograph of the underground structure and the designed extreme sections. Neoprene foams were used to allow deformation of tunnel extremities and the longitudinal sides of the ESB box were covered with Teflon sheets to reduce surface friction.

### *Instrumentation*

The instrumentation layout is presented in Fig. 3. Shear strains of the model ground were obtained using the data provided by accelerometers buried in the soil. The deformations formed in transverse direction were obtained by means of horizontal and diagonal extensometers placed into the underground structure model and particularly designed for the rectangular underground structure models. Figure 4 shows the pairs of horizontal extensometers reciprocally piled over a fork-shaped system. The horizontal deformations along the height of both sidewalls of the model were, thus, recorded correspondingly. To examine the boundary effects and to check the validity of plain strain conditions, four pieces of diagonal extensometers were used as shown in Fig. 4.

## CENTRIFUGE TEST RESULTS

Eight tests were performed in a centrifuge field of 40$\boldsymbol{g}$. Harmonic motions were executed with prototype accelerations of 0·25$\boldsymbol{g}$ and 0·40$\boldsymbol{g}$, and frequencies of 2 and 3·5 Hz, respectively. Each model was tested under four different

**Table 2.** Cross-section dimensions of underground structure models

| | Model 1 | | Model 2 | |
|---|---|---|---|---|
| | Internal dimensions | External dimensions | Internal dimensions | External dimensions |
| Model scale: mm | 38<br>44 | 50<br>50 | 38<br>44 | 50<br>54 |
| Prototype scale: m | 1·52<br>1·76 | 2·0<br>2·0 | 1·52<br>1·76 | 2·0<br>2·16 |

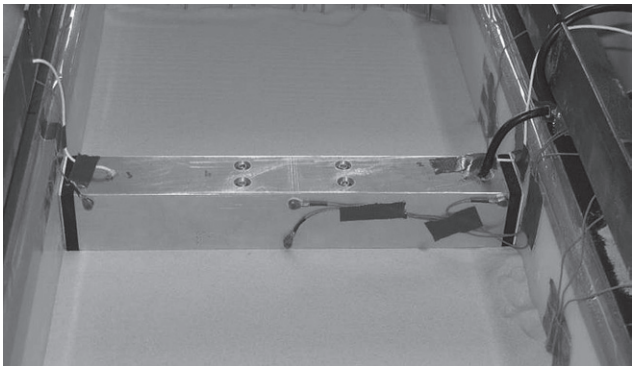

(a)

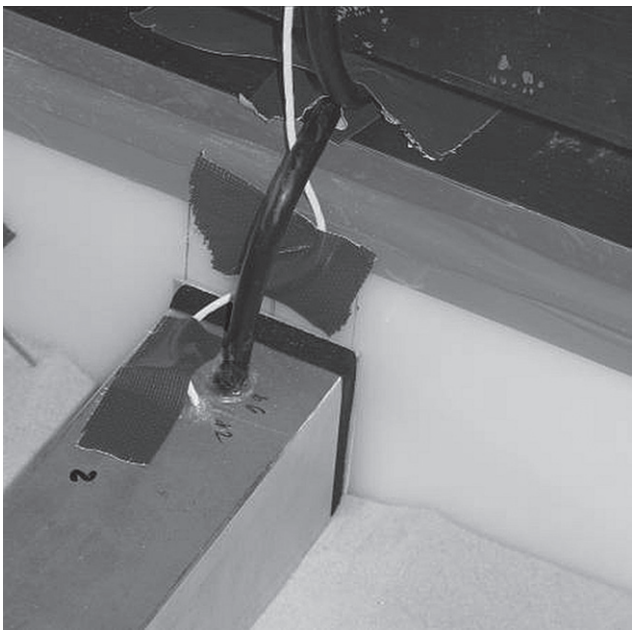

(b)

**Fig. 2.** Underground structure model: (a) general view; (b) closer view of extremity

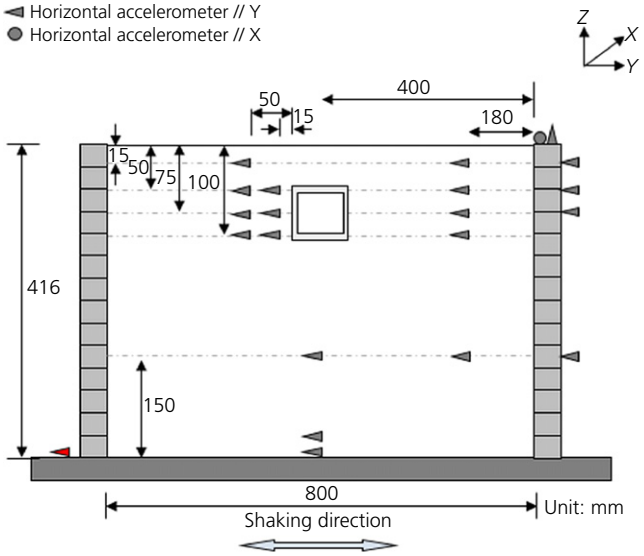


**Fig. 3.** Schematic illustration of test instrumentation

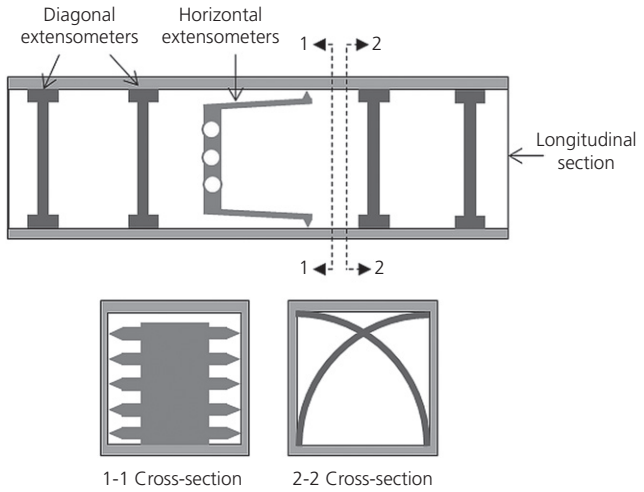


**Fig. 4.** Layout of extensometers placed inside the culvert model

harmonic motions as listed in Table 3. The measured accelerations are quite close to those targeted, but for the test numbered 9, ~20% higher base acceleration was recorded.

### *Soil response*

Maximum accelerations along the soil depth were normalised with maximum input acceleration and plotted as shown in Fig. 5. As seen from the figure, acceleration amplification gradually increases from base to 4 m below the surface and a sudden increase in amplification takes place near the surface. Furthermore, acceleration amplification decreases with increasing acceleration and frequency. Soil displacements were obtained by double integration of accelerometer records filtered between 20 and 600 Hz in model scale (0·5–15 Hz in prototype scale). Table 4 shows the shear strain values calculated at the mid-depth of underground structure model at different locations in the model ground. The accelerometers located farther from the culvert (180 mm away from ESB) were used to calculate free-field strains. As given in Table 4, there are only slight differences between the shear strains obtained at different locations. Shear strain values at 50 mm away from the underground structure model are almost equal to free-field

**Table 3.** Testing programme

| Test number | Underground structure model | Targeted input acceleration ($g$) (prototype) | Measured input acceleration ($g$) (prototype) | Frequency: Hz (prototype) | Duration: s (prototype) |
|---|---|---|---|---|---|
| 1 | Model 1 | 0·25 | 0·27 | 2 | 35·2 |
| 2 | Model 1 | 0·25 | 0·28 | 3·5 | 20 |
| 3 | Model 1 | 0·4 | 0·41 | 2 | 35·2 |
| 4 | Model 1 | 0·4 | 0·4 | 3·5 | 20 |
| 5 | Model 2 | 0·25 | 0·27 | 2 | 35·2 |
| 6 | Model 2 | 0·25 | 0·28 | 3·5 | 20 |
| 7 | Model 2 | 0·4 | 0·49 | 2 | 35·2 |
| 8 | Model 2 | 0·4 | 0·39 | 3·5 | 20 |

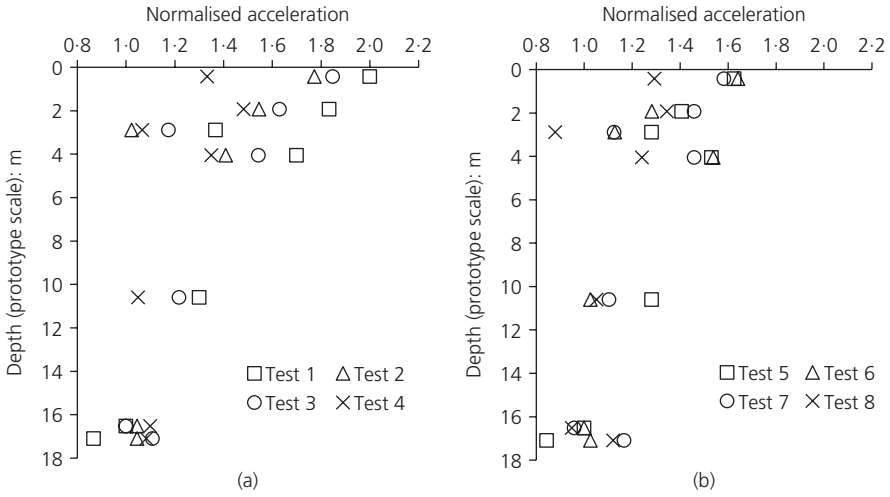


**Fig. 5.** Variation of maximum acceleration amplification along the depth of ground model

**Table 4.** Shear strain values at the mid-depth of underground structure models

| | Test 1 | Test 2 | Test 3 | Test 4 | Test 5 | Test 6 | Test 7 | Test 8 |
|---|---|---|---|---|---|---|---|---|
| 180 mm from ESB | 0·003 | 0·0018 | 0·0085 | 0·0035 | 0·0025 | 0·002 | 0·0087 | 0·0037 |
| 15 mm from culvert | 0·003 | 0·0018 | 0·0120 | 0·0040 | 0·0030 | 0·0021 | 0·0120 | 0·0040 |
| 50 mm from culvert | 0·003 | 0·0018 | 0·010 | 0·0038 | 0·0025 | 0·002 | 0·0085 | 0·0033 |

strains. Although the shear strains are mostly around 0·3%, maximum shear strains are exceeding 1% when the input motion has a prototype acceleration of more than 0·4$g$ and a frequency of 2 Hz. Li *et al.* (2013) stated that the resonant frequency of the model ground was ~3·5 Hz at low strain levels. It is observed that the strain level has a tendency of increasing when the model is vibrated with a frequency of 2 Hz. This may be due to a decrease in natural frequency of the model ground depending on the shear modulus degradation during the shaking process. Therefore, the non-linear behaviour of soil at large strains can shift the resonant frequency closer to 2 Hz.

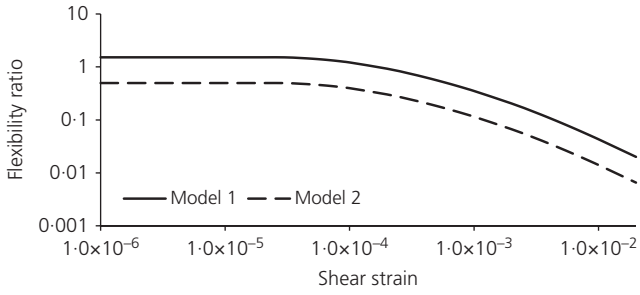


**Fig. 6.** Measured sidewall deformations for the two underground structure models: (a) tests 1 and 5; (b) tests 2 and 6; (c) tests 3 and 7; (d) tests 4 and 8

### *Sidewall deformations*

Wang (1993) quantified the relative racking stiffness by the flexibility ratio ($F$) and formulated as follows

$$F = \frac{G_m \times W}{\boldsymbol{S} \times H} \tag{5}$$

where $\boldsymbol{S}$ is the force required for unit racking deformation, $G_m$ is the degraded shear modulus and $W$ and $H$ are the width and height of the underground structure, respectively. Variation of flexibility ratio with respect to shear strain is given for the tunnel models in Fig. 6. Since the shear modulus is highly sensitive to shear strain level, an initial flexibility ratio, IF, is defined by replacing $G_m$ in equation (5), by $G_{max}$ as given in the following equation

$$\text{IF} = \frac{G_{max} \times W}{\boldsymbol{S} \times H} \tag{6}$$

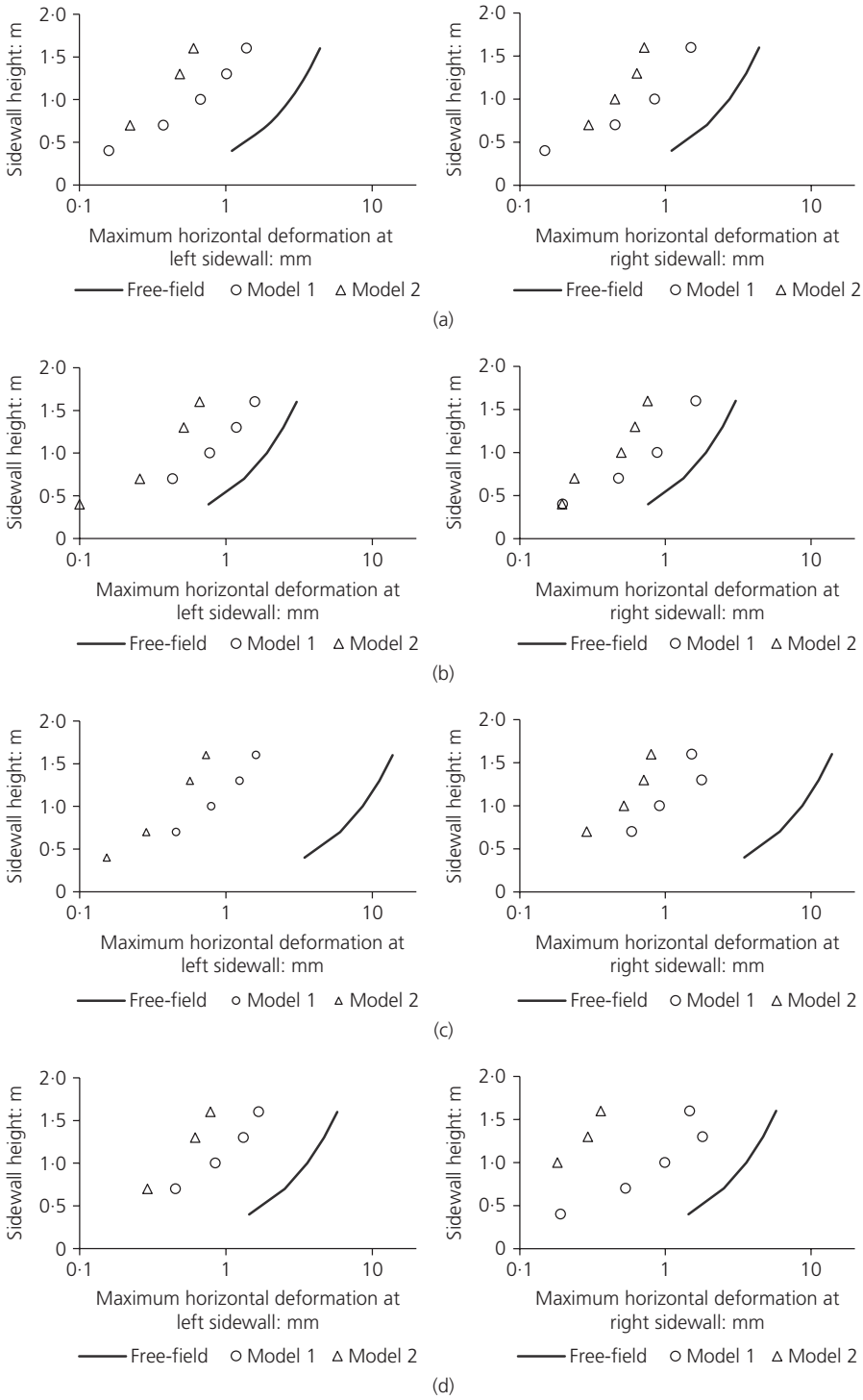


**Fig. 7.** Comparison between centrifuge test results and simplified frame analysis methodologies in terms of racking ratio

Lateral deformations of the buried structure models under dynamic loading were measured using extensometers mounted on sidewalls. Some data were missing due to measurement errors and instrument-related problems. Figure 7 shows the variation of maximum lateral deformation along the height of sidewalls. The measured maximum displacements at the top slab of model 1 were approximately twice that of model 2. Although free-field strains are much larger in tests 3 and 7 when compared with other model tests, there are only slight differences in underground structural strains.

As the racking of an underground structure is inherently related to soil–structure interaction, racking potential of such structures is mostly evaluated using the racking ratio, $R$, given by the following formula

$$R = \frac{\Delta_{\mathrm{str}}}{\Delta_{\mathrm{ff}}} \tag{7}$$

where $\Delta_{\mathrm{str}}$ is the racking deformation of the underground structure and $\Delta_{\mathrm{ff}}$ is the free-field deformation. Racking deformations of the tunnel models were directly measured using horizontal extensometers mounted in the models. Having computed the free-field deformations (obtained from accelerometer measurements) at mid-depth of the model structure, the racking ratios generated through centrifuge

testing were obtained. These results were compared with the predictions of analytical solutions proposed by Penzien (2000) and Bobet *et al.* (2008). Both approaches strongly depend on the relative stiffness between the soil and the underground structure. Therefore, comparison of the test and analytical results is given in terms of the relationship between $R$ and flexibility ratio ($F$) as presented in Fig. 8. Degraded shear modulus, $G_m$, has a major importance in calculating $F$ values. $G_m$ was estimated using $G_{max}$ (equation (1)), modulus degradation equations (equations (2)–(4)) and the obtained free-field strains from centrifuge tests. Racking ratios predicted by Penzien's approach are nearly half to two-third of those obtained from dynamic centrifuge tests. The approach proposed by Bobet *et al.* (2008) gives higher racking deformations when compared with Penzien's (2000) approach and overestimates the centrifuge results approximately by a factor between 2 and 3. The difference between the deformations estimated by these analytical approaches may be attributed to the principles featured in the procedures. In the approach by Penzien (2000), only shear stresses at the interface are taken into consideration and the effect of normal stress on racking deformation is entirely ignored. As the relative stiffness between the structure and soil decreases, the effect of normal stress on racking deformation increases. Moreover, the $G$ values obtained using modulus degradation equations were directly implicated in the procedure of Penzien (2000), whereas they were used as initial estimates of shear modulus in the procedure of Bobet *et al.* (2008). Bobet *et al.* (2008) suggest an iterative procedure to refine the shear modulus and the corresponding shear strain due to change of soil stiffness with structure deformation.

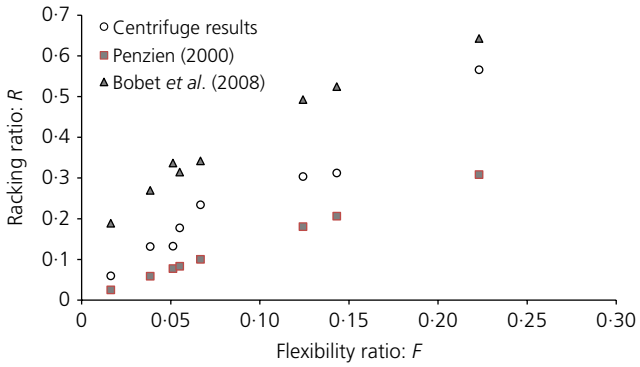


**Fig. 8.** Variation of flexibility ratio with respect to shear strain

### *Dynamic lateral earth pressures*

It is very difficult to determine the theoretical pressure distribution (Fig. 9(a)) acting on the underground structure. Wang (1993) recommended pseudo-triangular pressure distribution for shallow rectangular underground structures subjected to dynamic loading as illustrated in Fig. 9(b). Using this assumption, the maximum pressure value at the upper corner of the embedded structure is denoted by $P_d$. It should be noted that the deformation of top corner is maximum; the pressure at top corner is just the maximum value of the assumption. In other words, the pressure acting on the top corner is not necessarily the largest value.

Pseudo-triangular pressure distribution was applied to underground structure models and the required $P_d$ values for racking deformations measured in centrifuge tests were determined by back calculation. To obtain dynamic lateral pressure coefficient, $k_d$, the $P_d$ value is normalised with the overburden pressures at the mid-depth of the tunnel ($\sigma'_{v,mid}$) as given in the following equation

$$k_d = \frac{P_d}{\sigma'_{v,mid}} \tag{8}$$

The $k_d$ values obtained from the present study and Ulgen *et al.* (2015) were plotted against IF and $F$ in Figs 10 and 11, respectively. They increase with increasing rigidity of the structure and vary between ~0·4 and 2. This $k_d$ value may be used in the preliminary seismic assessment of box-type rigid underground structures buried in dry sand. However, more experimental research is needed to estimate $k_d$ values with reasonable accuracy for different structural rigidities.

## CONCLUSIONS

In this study, a series of dynamic centrifuge tests were performed on two rectangular sectioned tunnel models in dry sand under 40***g*** of centrifugal acceleration. The following conclusions are drawn from the test results.

(*a*) A comparison between the centrifuge tests results and Penzien's estimates show that racking ratios were underestimated nearly by a factor of 1·5–2 using Penzien's approach. This underestimation may be due to the ignorance of dynamic soil pressures.

(*b*) Racking ratios obtained from centrifuge tests are overestimated by roughly a factor between 2 and 3 using the method of Bobet *et al.* Thus, the racking deformation calculated by the approach proposed by Bobet *et al.* may be used as a conservative estimate in the preliminary design of box-type rigid rectangular underground structures embedded in dry sand.

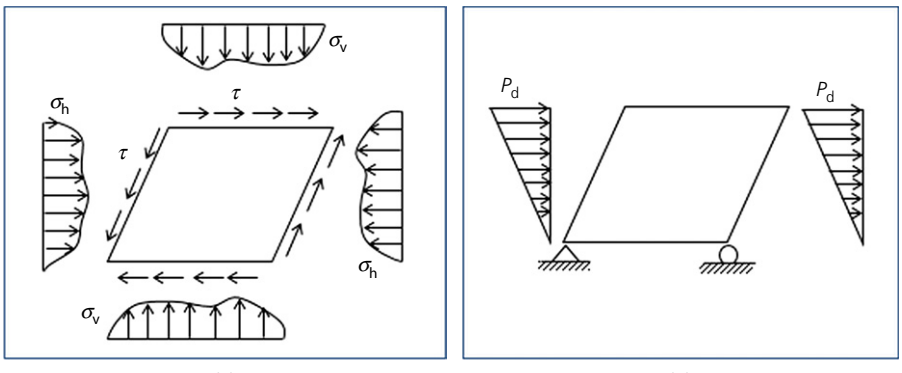


**Fig. 9.** Dynamic pressure distribution acting on a rectangular underground structure: (a) theoretical pressure distribution; (b) simplified pressure distribution (Wang, 1993)

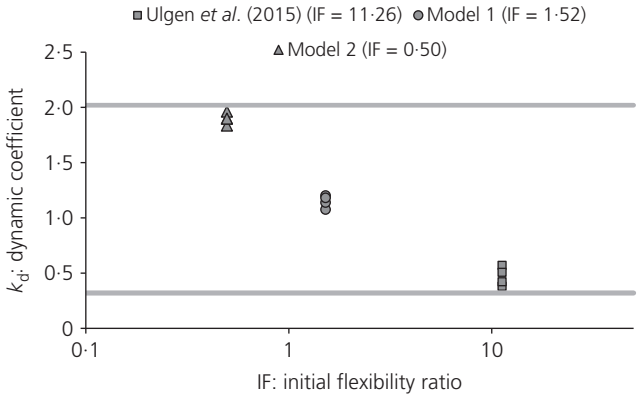


**Fig. 10.** Dynamic lateral coefficient $k_d$ against IF

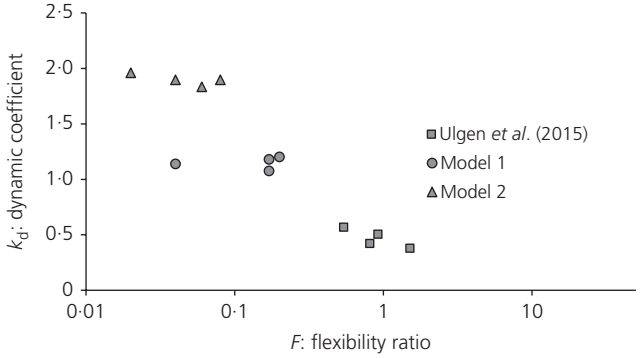


**Fig. 11.** Dynamic lateral coefficient $k_d$ against $F$

(*c*) The $k_d$ value increases with increase of tunnel stiffness and varies between ~0·4 and 2. This coefficient may help to carry out a preliminary design for the box-type rigid underground structures buried in dry sand under seismic loading. However, further experimental studies are needed to obtain $k_d$ values for underground structures with different rigidities.

## ACKNOWLEDGEMENTS

This research has received funding from the European Union Seventh Framework Programme (FP7/2007–2013) under the grant agreement no. 227887 (SERIES). The authors thank IFSTTAR centrifuge team for their valuable supports throughout the study.

## REFERENCES

Bobet, A., Fernández, G., Huo, H. & Ramírez, J. (2008). A practical iterative procedure to estimate seismic induced deformations of shallow rectangular structures. *Canadian Geotech. J.* **45**, No. 7, 923–938.

Chian, S. C. & Madabhushi, S. P. G. (2012). Effect of buried depth and diameter on uplift of underground structures in liquefied soils. *J. Soil Dyn. Earthq. Eng.* **41**, No. 1, 181–190.

Cilingir, U. & Madabhushi, S. P. G. (2011a). Effect of depth on the seismic response of circular tunnels. *Can. Geotech. J.* **48**, No. 1, 117–127.

Cilingir, U. & Madabhushi, S. P. G. (2011b). A model study on the effects of input motion on the seismic behavior of tunnels. *J. Soil Dyn. Earthq. Eng.* **31**, No. 3, 452–462.

Cilingir, U. & Madabhushi, S. P. G. (2011c). Effect of depth on the seismic response of square tunnels. *Soils Found.* **51**, No. 3, 449–457.

Dashti, S., Hushmand, A., Ghayoomi, M., McCartney, J. S., Zhang, M., Hushmand, B., Mokarram, N., Bastani, A., Davis, C., Yangsoo, L. & Hu, J. (2013). Centrifuge modeling of seismic soil–structure-interaction and lateral earth pressures for large near-surface underground structures. *Proceedings of the 18th international conference on soil mechanics and geotechnical engineering*, Paris, pp. 899–902.

Ha, D., Abdoun, T. H., O'Rourke, M. J., Symans, M.D., O'Rourke, T. D., Palmer, M. C. & Stewart H. E. (2010). Earthquake faulting effects on buried pipelines-case history and centrifuge study. *J. of Earthq. Eng.* **14**, No. 5, 646–669.

Hardin, B. O. & Drnevich, V. P. (1972). Shear modulus and damping in soils: design equation and curves. *J. Soil Mech. Found. Engng Div., ASCE* **98**, No. 7, 667–692.

Hashash, Y. M., Hook, J. J., Schmidt, B. & IChiang Yao, J. (2001). Seismic design and analysis of underground structures. *Tunnelling and Underground Space Tech.* **16**, No. 4, 247–293.

Huo, H., Bobet, A., Fernandez, G. & Ramirez, J. (2006). Analytical solution for deep rectangular underground structures subjected to far field shear stresses. *Tunnelling and Underground Space Tech.* **21**, No. 6, 613–625.

Iida, H., Hiroto, T., Yoshida, N. & Iwafuji, M. (1996). Damage to Daikai subway station. *Soils Found.* **36**, No. S (Special issue), 283–300.

Ishibashi, I. & Zhang, X. (1993). Unified dynamic shear moduli and damping ratios of sand and clay. *Soils Found.* **33**, No. 1, 182–191.

Kaneshiro, J. Y., Power, M. & Rosidi, D. (2000). Empirical correlations of tunnel performance during earthquakes and aseismic aspects of tunnel design. *Proceedings of the conference on lessons learned from recent earthquakes – on earthquakes in Turkey 1999*, 8–11 November.

Lanzano, G., Bilotta, E., Russo, G., Silvestri, F. & Madabhushi, S. P. G. (2012). Centrifuge modeling of seismic loading on tunnels in sand. *Geotech. Testing J.* **35**, No. 6, 854–869.

Lee, S. H., Choo, Y. W. & Kim, D. S. (2013). Performance of an equivalent shear beam (ESB) model container for dynamic geotechnical centrifuge tests. *J. Soil dyn and Earthq. Eng.* **44**, No. 1, 102–114.

Li, Z., Escoffier, S. & Kotronis, P. (2013). Using centrifuge tests data to identify the dynamic soil properties: application to Fontainebleau sand. *Soil Dyn. Earthq. Engng* **52**, 77–87.

Ling, H. I., Mohri, Y., Kawabati, T., Liu, H., Burke, C. & Sun, L. (2003). Centrifugal modeling of seismic behavior of large-diameter pipe in liquefiable soil. *J Geotech Geoenviron Eng* **129**, No. 12, 1092–1101.

Madabushi, S. P. G. (1994). *Dynamic response of the equivalent shear beam (ESB) container*, Technical Report TR270. Cambridge, UK: Department of Engineering, University of Cambridge.

O'Rourke, M., Gadicherla, V. & Abdoun, T. (2003). Centrifuge modeling of buried pipelines. *Proceedings of the 6th U.S. conference and workshop on lifeline earthquake engineering*, California, pp. 757–768.

Pitilakis, K., Tsinidis, G., Anastisiadis, A., Pitilakis, D., Heron, C., Madabushi, S. P. G., Stringer, M. & Paolucci, R. (2013). Investigation of several aspects affecting the seismic behaviour of shallow rectangular underground structures in soft soils, Final Report, Series: Seismic engineering research infrastructures for European synergies, Series Project Web. http://www.series.upatras.gr/sites/default/files/file/SERIES_TUNNELSEIS_Final_Report.pdf.

Penzien, J. (2000). Seismically induced racking of tunnel linings. *Earthq. Engng Struct. Dyn.* **29**, No. 5, 683–691.

Power, M., Rosidi, D. & Kaneshiro, J. (1998). Seismic vulnerability of tunnels and underground structures revisited. *Proceedings of the North American Tunneling Conference*, California, pp. 243–250.

Sitar, N. (1995). *Geotechnical reconnaissance of the effects of the January 17, 1995, Hyogoken-Nanbu earthquake, Japan*. Earthquake Engineering Research Center, University of California, Berkeley, CA, USA, Report No. 95-01.

St. John, C. M. & Zahrah, T. F. (1987). Aseismic design of underground structures. *Tunnelling Underground Space Technol.* **2**, No. 2, 165–197.

Teymur, B. & Madabhushi, S. P. G. (2003). Experimental study of boundary effects in dynamic centrifuge modelling. *Geotechnique*

**53**, No. 7, 655–663, http://dx.doi.org/10.1680/geot.2003.53.7.655.

Ulgen, D., Saglam, S. & Ozkan, M. Y. (2015). Dynamic response of a flexible rectangular underground structure in sand: centrifuge modeling. *Bull. of Earthq. Eng.* **13**, No. 9, 2547–2566.

Wang, J. N. (1993). *Seismic design of tunnels: a state of the art approach*, Monograph 7. New York, NY, USA: Parsons Brinckerhoff Quade & Douglas Inc.

Wang, W. L., Wang, T. T., Su, J. J., Lin, C. H., Seng, C. R. & Huang, T. H. (2001). Assessment of damage in mountain tunnels due to the Taiwan Chi Chi Earthquake. *Tunnelling Underground Space Technol.* **16**, No. 3, 133–150.

Zeng, X. & Schofield, A. N. (1996). Design and performance of an equivalent-shear-beam container for earthquake centrifuge modelling. *Geotechnique* **46**, No. 1, 83–102, http://dx.doi.org/10.1680/geot.1996.46.1.83.